European Journal of Environmental and Civil Engineering

ISSN: 1964-8189 (Print) 2116-7214 (Online) Journal homepage: http://www.tandfonline.com/loi/tece20

Design graphs to estimate reduction factor of nonwoven geotextiles due to installation process

Gh. Tavakoli Mehrjardi & E. Amjadi Sardehaei

To cite this article: Gh. Tavakoli Mehrjardi & E. Amjadi Sardehaei (2017): Design graphs to estimate reduction factor of nonwoven geotextiles due to installation process , European Journal of Environmental and Civil Engineering, DOI: 10.1080/19648189.2017.1327897

To link to this article: http://dx.doi.org/10.1080/19648189.2017.1327897

EUROPEAN JOURNAL OF ENVIRONMENTAL AND CIVIL ENGINEERING, 2017
https://doi.org/10.1080/19648189.2017.1327897

Design graphs to estimate reduction factor of nonwoven geotextiles due to installation process

Gh. Tavakoli Mehrjardi and E. Amjadi Sardehaei

Department of Civil Engineering, Faculty of Engineering, Kharazmi University, Tehran, Iran

ABSTRACT

It seems that performance of geotextiles is directly related to their survivability, which affects design economy. This paper aims to present design graphs in order to estimate the tensile strength reduction factors of nonwoven geotextiles due to the installation process in the soil embankment. The design graphs have been established based on a series of full-scale field tests and analytical procedures. The variables include medium grain size of backfill materials, subgrade CBR, relative density of backfills, as-received geotextile tensile strength and the transferred stress over the geotextiles level, during installation. It is concluded that tensile strengths of the geotextile got decreased in the aftermath of compaction process under higher relative density, larger particle size of the backfill, lower as-received grab tensile strength (decreasing the AASHTO's geotextiles class from 1 to 3) and finally, being in the neighbourhood of weaker subgrades. These intensifying conditions necessitate designers using high-survivability geotextiles.

ARTICLE HISTORY
Received 27 November 2016
Accepted 27 April 2017

KEYWORDS
Installation damage; geotextiles; grab tensile strength; retained tensile strength; reduction factor

1. Introduction

Reinforced soils offer economy, ease of installation, performance and reliability in many areas of geotechnical engineering. Using planar reinforcement, especially geotextiles, can enhance bearing capacity and reduce settlement of foundation beds (Becker & Da silva Nunes, 2015; Costa, Zornberg, Bueno, & Costa, 2016; Hosseinpour, Almeida, & Riccio, 2015; Portelinha, Bueno, & Zornberg, 2013; Portelinha, Zornberg, & Pimentel, 2014; Tavakoli Mehrjardi, Ghanbari, & Mehdizadeh, 2016; Tavakoli Mehrjardi, Moghaddas Tafreshi, & Dawson, 2013; Wang, Zhang, & Zhang, 2011).

Selecting a geotextile for either permanent or temporary roads depends upon the survivability criteria. In fact, the stresses applied to the subgrade and the geotextile during construction may be much greater than those applied in service. Therefore, selection of the geotextile in roadway applications is usually governed by the anticipated construction stress. In other words, the geotextile must survive the construction operations if it is to perform its intended function (Holtz, Christopher, & Berg, 1998).

Revision of previous research clarifies that installation damage of geotextiles in reinforced-soil structures can be evaluated through the field or laboratory tests. In fact, after completion of the installation process, the samples are exhumed and the physical and mechanical properties are examined by visual inspection and tensile strength tests.

CONTACT Gh. Tavakoli Mehrjardi ghtavakoli@khu.ac.ir

In visual inspection, two methods including the scanning electron microscopy (SEM) and evaluated with the naked eye are applicable. For these major, different modes of installation outcomes such as cutting, fraying, very fine-grained particles sediment in texture, fibre separation, holes and squeeze of geotextiles by larger soil particles are investigated. Greenwood and Brady (1992), based on visual inspections by the SEM method, stated that damage modes generally involved cutting, fraying (decay) and erosion. Pinho-Lopes and Lopes (2013) reported cutting and puncture as damage modes. Furthermore, Rosete et al. (2015) observed fine-grained particles sediment in texture of geotextile. Also, Carlos, Pinho-Lopes, Carneiro, and Lopes (2015) pointed out that finer soils (silty sand and sandy silt) created less visible changes (without fibre separation, cutting and erosion) and granular soils (sand and gravel) exerted fibre separation and fibre-cutting.

Importance of having a safe and, of course, economical design of reinforced embankments necessitates the designers to select a proper tensile strength for geotextile. To do so, comparison of the geotextiles strength before (as-received) with after (remained) installation is inevitable. It is possible that the strength of exhumed samples from the field tests evaluates with tensile strength tests encompassing grab tensile strength and wide-width tensile strength. Many researchers studied the tensile behaviour of geotextiles during the installation process and evaluated the effect of different parameters such as energy absorption potential, medium grain size of backfill materials, angularity of backfill materials, subgrade's type of geotextile, compaction energy, type of geotextile and thickness of the top layer on geotextile. Brief descriptions of the obtained results, presented by previous researchers, are tabulated in Table 1. This table shows how the geotextile behaved under increasing the specific parameter. For instance, Nikbakht and Diederich (2008) used the area under the stress–strain curve in wide-width tensile test as energy absorption of geotextiles. They showed that the retained strength increased (or reduction factor decreased) by increasing geotextile properties such as its thickness and as-received tensile strength.

Although, there have been many studies into the installation damage of geotextiles, there is a lack of investigation into the response of geotextiles after installation with respect to a package of different parameters such as aggregate size, subgrade's stiffness, relative density of the backfill and different classes of geotextiles. This study aims to introduce a design graph, focused on the practical aspects of design in road construction, derived from an analytical approach based on a series of full-scale field tests. Also, some useful recommendations in proper estimation of allowable tensile strength for geotextiles are presented.

2. Experimental studies

A series of full-scale field tests were carried out to investigate installation damage of geotextiles in unpaved roads. Four types of uniformly graded soils as backfill materials with the medium grain size of 3, 6, 12 and 16 mm were considered. Two types of well-graded course materials namely "fine-grained subgrade, FS" and "coarse-grained subgrade, CS" are used to simulate the subgrade of backfill materials. The properties of these backfill and subgrade materials have been summarised in Table 2. Also, the grading of backfill materials is graphically illustrated in Figure 1.

Also, three types of needle-punched nonwoven geotextiles, made of polypropylene, are used to be representatives of classes 1, 2 and 3 in accordance with American Association of State Highway and Transportation Officials (AASHTO M 288-08). Engineering properties of the geotextiles are provided in Table 3.

In order to simulate installation process of geotextiles in unpaved roads, a physical model was developed at Kharazmi University. Figure 2 shows the test set-up, having inside dimensions of 9000 × 2350 mm in plan (longitudinal and transversal directions, respectively). This area was divided by two kinds of subgrades, namely "FS" and "CS", in order to attain soft and stiff subgrades, respectively. The subgrades were constructed in a layer of 150 mm-lift thickness, having 5% water content to achieve the relative density of 95%, at least. According to Figure 2(b), the mentioned area was surrounded by concrete frame supported by buttresses, having thickness and depth of 150 mm, to prevent spreading

Table 1. Summarised obtained results, presented by previous researchers, on installation damage of geotextile.

Parameter								
Research type	Researchers	Energy absorption potential	Medium grain size of backfill materials	Angularity of backfill materials	Subgrade type of geotextile	Compaction energy	Geotextile class	Thickness of the top layer on geo-textile
Field	Koerner and Koerner (1990)	NI*	Damage increased	NI	Damage increased	Damage increased	NI	Damage increased
	Greenwood and Brady (1992)	NI	Damage increased	NI	NI	Damage increased	NI	NI
	Watn et al. (1998)	NI	NI	NI	NI	Damage increased	Damage decreased	NI
	Richardson (1998)	NI	Damage increased	NI	NI	NI	Damage decreased	Damage decreased
	Elias (2001)	NI	Damage increased	NI	NI	NI	NI	NI
	Nikbakht and Diederich (2008)	Damage decreased	NI	NI	NI	NI	Damage decreased	NI
Laboratory	Elvidge and Raymond (1999)	NI	Damage increased	NI	NI	Damage increased	Damage decreased	NI
	Mendes, Palmeira, and Matheus (2007)	NI	Damage increased	NI	NI	NI	NI	NI
	Rosete et al. (2013)	NI	NI	NI	NI	NI	Damage decreased	NI
	Carlos et al. (2015)	NI	Damage increased	NI	NI	NI	Damage decreased	NI
Field-laboratory	Pinho-Lopes and Lopes (2013)	NI	Damage increased	NI	NI	Damage increased	Damage decreased	NI
	Hufenus et al. (2005)	NI	Uncertainty	Uncertainty	Uncertainty	Damage increased	NI	NI

*NI: Not investigated.

Table 2. Physical properties of backfill materials and subgrades.

	Backfill materials				Subgrade	
Description	Sand 3 mm	Gravel 6 mm	Gravel 12 mm	Gravel 16 mm	CS (0–2 mm)	FS (0–25 mm)
Coefficient of uniformity, C_u	2.125	2.14	1.33	1.27	10.95	7.16
Coefficient of curvature, C_c	1.19	1.08	0.95	0.96	2.86	1.55
Medium grain size, D_{50} (mm)	3.1	5.9	12.5	16.5	3.65	1.00
Specific gravity, G_s	2.419	2.494	2.546	2.604	___	___
CBR soaked (%)	___	___	___	___	49	27
Moisture content (%)	Dry	Dry	Dry	Dry	5	5
Classification (USCS)	SP	GP	GP	GP	SW	SW

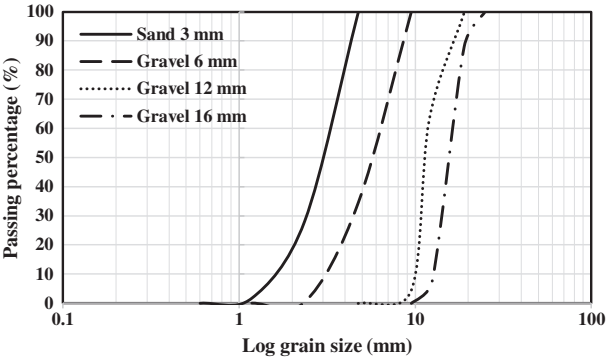

Figure 1. Grain size distribution curves for backfill materials.

of the backfill during compaction process. In all installations, firstly, both subgrades were successively covered by geotextiles class 1, 2 and 3 with dimensions of 1000 × 1200 mm. Then, one of the backfill materials was poured into the frame and above the geotextiles in layers of 50 mm-lift thickness to reach 100 mm height. In order to compact the backfill, a walk-behind tandem vibratory roller was utilised to achieve the desired relative density (D_r = 70% (medium dense) or 90% (very dense)) of the soils. Finally, at the end of compaction process, the backfill dug out carefully and the geotextiles were exhumed with caution and without any additional damages.

For easy recognition of a test, a system of coding with presence of A-B-C-D was defined. This is decoded in the way that "A" mentions class of the geotextiles, "B" mentions subgrades' type, "C" points out backfill materials and "D" means the relative density of backfill. For example, the test with codes of GT_1-CS-6-C_1 and GT_3-FS-3-C_2 means that the geotextile class 1 has been installed on coarse-grained subgrade and has backfill with D_{50} = 6 mm, compacted with D_r = 70%, at the top and the geotextile class 3 has been installed on fine-grained subgrade and has backfill with D_{50} = 3 mm, compacted with D_r = 90%, at the top, respectively. In order to assess the reliability of the results and finally to verify the consistency of the test data, many of the tests, described in Table 4, were repeated at least twice. The results obtained revealed a close match between results of the two trial tests with maximum differences in results of around 9%.

Grab tensile strengths of the exhumed geotextiles were assessed, according to American Society for Testing and Materials (ASTM D4632-15), to quantify damage severity of the geotextiles, in the aftermath of installation in the backfill. To do so, specimens of geotextiles with dimensions of 203.2 × 101.6 mm were punched from its sample. Then, having got the free distance of 75 mm between the clamps, the tensile testing machine started tensile loading at rate of 300 mm/min till rupture took place. During the

Table 3. Engineering properties of the geotextiles used.

Description	GT_3	GT_2	GT_1
Mass per unit area (gr/m^2)	292	319	508
Thickness (mm)	1.2	2	3.2
Apparent opening size (mm)	0.25	0.2	0.15
Grab tensile strength (N)	650	800	1350
Grab elongation (%)	> 50	> 50	> 50
Trapezoidal tear strength (N)	310	385	600
CBR puncture (N)	900	1500	2500
Class (AASHTO M 288–08)	3	2	1

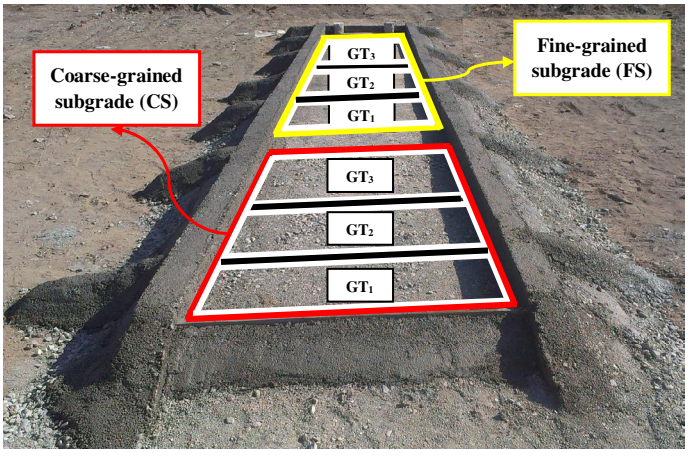

(a)

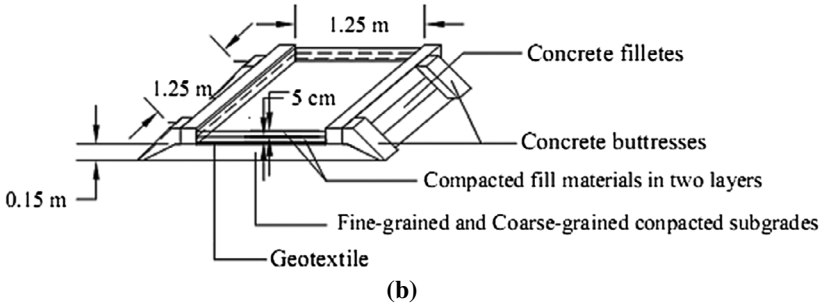

(b)

Figure 2. The test setup plan (a) reality (longitudinal) (b) schematic (transversal direction).

test, grab tensile forces accompanied with corresponding elongations were simultaneously recorded. Table 4 allows comparing the values of grab tensile strength obtained in each test condition.

To evaluate the response of geotextiles during elongation, the load–strain curves of geotextile specimens of classes 1, 2 and 3, before and after installation are compared in Figure 3. The retained curves belonged to the samples installed on coarse-grained subgrade and has backfill with D_{50} = 16 mm, compacted with D_r = 90%, at the top.

As can be seen in Figure 3, irrespective to the geotextiles' class, the tensile strength after installation got reduced in compared with as-received status. In fact, depending on the installation process, construction of the backfill causes the geotextile damage, tending to tensile strength reduction. Also, the installation process resulted in decreasing the failure strain of geotextiles after installation. On other

Table 4. Values of retained grab tensile strength obtained in each test condition.

Test code	Tensile strength (N)	Specimen code	Tensile strength (N)	Specimen code	Tensile strength (N)
GT_1-CS-3-C_1	1321	GT_2-FS-6-C_1*	666	GT_3-CS-12-C_2	575
GT_2-CS-3-C_1	893	GT_3-FS-6-C_1	690	GT_1-FS-12-C_2	1206
GT_3-CS-3-C_1*	599	GT_1-CS-6-C_2	1243	GT_2-FS-12-C_2	695
GT_1-FS-3-C_1*	1397	GT_2-CS-6-C_2*	662	GT_3-FS-12-C_2	704
GT_2-FS-3-C_1	743	GT_3-CS-6-C_2	605	GT_1-CS-16-C_1*	1459
GT_3-FS-3-C_1	633	GT_1-FS-6-C_2	1325	GT_2-CS-16-C_1	920
GT_1-CS-3-C_2	1332	GT_2-FS-6-C_2	659	GT_3-CS-16-C_1	604
GT_2-CS-3-C_2*	887	GT_3-FS-6-C_2	615	GT_1-FS-16-C_1	1222
GT_3-CS-3-C_2	676	GT_1-CS-12-C_1	1333	GT_2-FS-16-C_1*	704
GT_1-FS-3-C_2	1289	GT_2-CS-12-C_1*	848	GT_3-FS-16-C_1*	538
GT_2-FS-3-C_2	755	GT_3-CS-12-C_1	599	GT_1-CS-16-C_2	1286
GT_3-FS-3-C_2	644	GT_1-FS-12-C_1	1387	GT_2-CS-16-C_2	597
GT_1-CS-6-C_1	1283	GT_2-FS-12-C_1	725	GT_3-CS-16-C_2	578
GT_2-CS-6-C_1*	731	GT_3-FS-12-C_1	658	GT_1-FS-16-C_2	1416
GT_3-CS-6-C_1	632	GT_1-CS-12-C_2	1375	GT_2-FS-16-C_2*	823
GT_1-FS-6-C_1	1237	GT_2-CS-12-C_2*	750	GT_3-FS-16-C_2	634

*The tests which were performed twice to confirm repeatability of the tests.

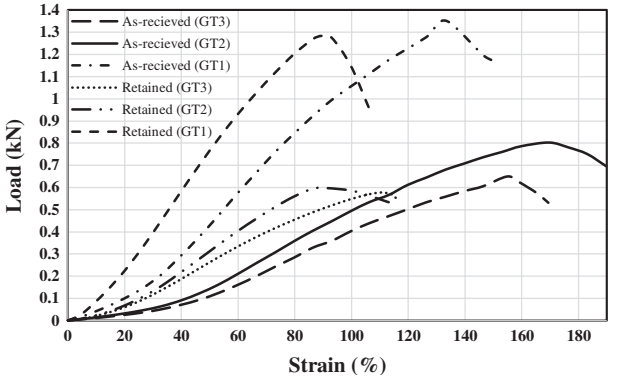

Figure 3. Load–strain curves of geotextiles specimens with classes 1, 2 and 3, before and after installation (retained samples with codes GT_3-CS-16-C_2, GT_2-CS-16-C_2 and GT_1-CS-16-C_2).

hand, it seems that the secant modulus of the geotextiles has been improved through the installation process. This may be owing to the fine-particle sediment in the texture of the geotextiles.

To see more details for values of the secant modulus as a representative of the geotextiles' stiffness, variations of the ratio of retained strength ($R = T_{ID} / T_0$) versus the ratio of retained stiffness (J_{ID} / J_0) at strain levels of 2%, 50% and failure for all specimens are illustrated in Figure 4. From this figure, it is concluded that the geotextiles became stiffer as they were elongated during the tensile tests. This is conceivably because of the fact that the samples experienced the loading–unloading–reloading conditions during installation–exhumation–tension process, respectively. Also, it is aforementioned that sediment of fine-grained particles reduced the porosity of the geotextiles, tending to behave as stiffer materials. Interestingly, the lighter geotextiles (class 2 and 3) had higher retained secant modulus due to absorbing more fine particles during installation because of larger initial porosity. Allen and Bathurst (1994) assessed short-term effects of installation damage on retained tensile strength of the geotextile and its modulus. They explained that premature failure at reduced strain had been encountered in the aftermath of local increases in stress owing to local defects of "notching" in the fibres, immediately after installation, although polymer material properties, such as modulus, were unchanged. They, also, certified that if significant numbers of fibres or ribs were severely damaged, however, stress levels in adjacent ribs or fibres became elevated and this damage is manifest as a decrease in the gross modulus of the material.

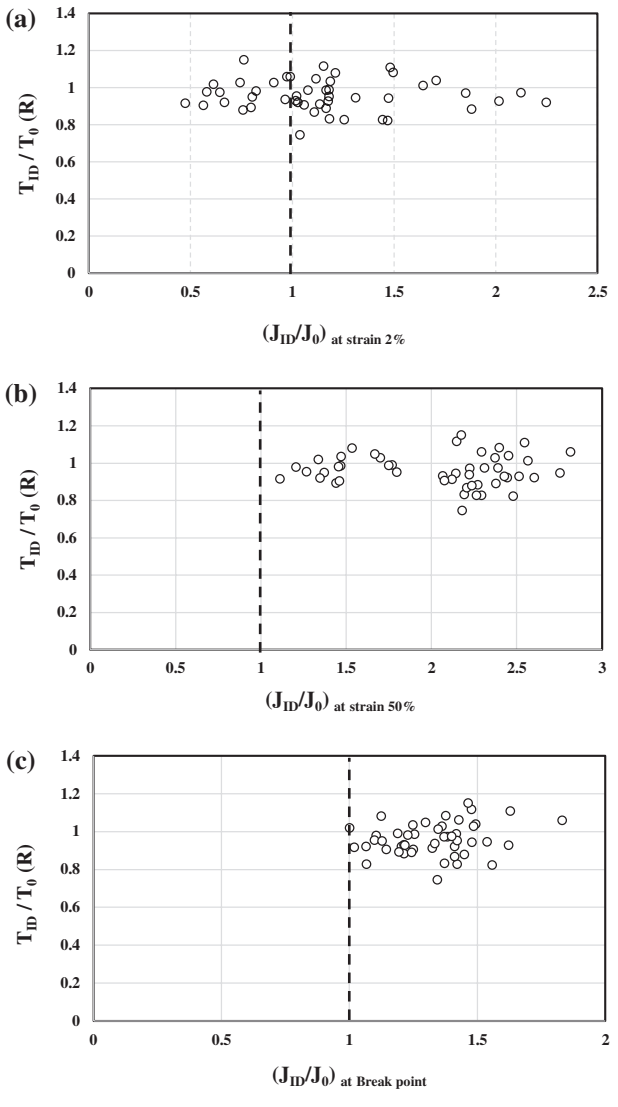

Figure 4. The chart of retained secant modulus ratio against retained strength ratio (R).

It should be notified that, to have a better assessments, all the samples, before and after installations, were scanned and some image processes were carried out. According to the visual inspections, none of fraying, fibre separation and holes were observed. However, in all specimens, fine-grained particles with a size of about 0 to 2 mm penetrated into the texture of the geotextiles. Although, the aggregates could not puncture the geotextiles, but, backfills with larger particles, especially for medium grain size of 12 and 16 mm, squeezed into the texture, specifically in geotextiles class 2 and 3. It should be added that one of main reasons for absence of severe damages was due to not using heavy compactor. Watn, Eiksund, and Knutson (1998) reported that numbers and size of the holes were significantly reduced in which lighter compactors were applied.

3. Analytical approach

Dimensional analysis has been taken to relate the studied parameters based on the acquired experimental results. Equations (1) and (2) illustrate dimensional and non-dimensional relationships to interpolate and extrapolate the effective parameters and remained tensile strength of the geotextiles (T_{ID}). According to Equation (1), the major physical parameters influencing the retained tensile strength (T_{ID}) can be summarised in medium grain size of backfill materials (D_{50}) in metre, subgrade CBR in term of percentage, relative density of backfills (D_r) in term of percentage, as-received geotextile tensile strength (T_0) in Newton and the transferred stress over the geotextiles level during installation (σ) in Pascal. Equation (1) comprises five parameters in which two of them have fundamental dimensions (i.e. length and force). Therefore, Equation (1) can be reduced to three independent parameters and substituted with Equation (2), where T_{ID} is retained grab tensile strength of geotextiles in (*N*); T_0 is as-received grab tensile strength of geotextiles in (*N*); σ is transferred stress at the level of geotextile in (Pa); D_{50} is medium grain size of the backfill in (m); D_r is relative density of the backfill in per cent and CBR is California bearing ratio of the subgrade in per cent.

$$T_{ID} = f(D_{50}, CBR, D_r, T_0, \sigma) \tag{1}$$

$$\frac{T_{ID}}{T_0} = f\left(\frac{T_0}{\sigma D_{50}^2}, D_r, CBR\right) \tag{2}$$

Table 5. Comparison of the results obtained by tests and regression models.

	RF_{ID}		
Test code	Grab tensile test	Regression models	Residual value
GT_1-CS-3-C_1	1.02	1.03	0.01
GT_3-CS-3-C_1	1.09	1.05	0.04
GT_2-FS-3-C_1	1.08	1.05	0.02
GT_3-FS-3-C_1	1.03	1.06	0.03
GT_1-CS-3-C_2	1.01	1.04	0.03
GT_1-FS-3-C_2	1.05	1.05	0.01
GT_2-FS-3-C_2	1.06	1.07	0.01
GT_3-FS-3-C_2	1.01	1.07	0.06
GT_1-CS-6-C_1	1.05	1.06	0.01
GT_2-CS-6-C_1	1.10	1.08	0.02
GT_3-CS-6-C_1	1.03	1.08	0.05
GT_1-FS-6-C_1	1.09	1.07	0.02
GT_2-FS-6-C_1	1.20	1.09	0.11
GT_1-CS-6-C_2	1.09	1.07	0.01
GT_2-CS-6-C_2	1.21	1.09	0.12
GT_3-CS-6-C_2	1.07	1.09	0.02
GT_1-FS-6-C_2	1.02	1.09	0.07
GT_2-FS-6-C_2	1.21	1.10	0.12
GT_3-FS-6-C_2	1.06	1.10	0.05
GT_1-CS-12-C_1	1.01	1.09	0.08
GT_3-CS-12-C_1	1.09	1.11	0.03
GT_2-FS-12-C_1	1.10	1.12	0.02
GT_2-CS-12-C_2	1.07	1.12	0.05
GT_3-CS-12-C_2	1.13	1.12	0.01
GT_1-FS-12-C_2	1.12	1.12	0
GT_2-FS-12-C_2	1.15	1.13	0.02
GT_3-CS-16-C_1	1.08	1.12	0.05
GT_1-FS-16-C_1	1.11	1.12	0.01
GT_2-FS-16-C_1	1.14	1.13	0.01
GT_3-FS-16-C_1	1.21	1.14	0.07
GT_1-CS-16-C_2	1.05	1.12	0.07
GT_2-CS-16-C_2	1.34	1.13	0.21
GT_3-CS-16-C_2	1.12	1.14	0.01
GT_3-FS-16-C_2	1.03	1.15	0.12

Several types of mathematical functions including cubic, quadratic, logarithmic, linear and exponential functions have been studied to select a regression model with the highest fitness, besides having the best significance. Among all possibilities, natural-logarithm function was chosen (see Equation (3)) to correlate the installation damage reduction factor (RF_{ID}) with the mentioned non-dimensional independent parameters.

$$RF_{ID} = \frac{T_0}{T_{ID}} = 1.09 - 0.023 \ln\left(\frac{T_0}{\sigma D_{50}^2}\right) + 0.046 \ln\left(D_r\right) - 0.02 \ln(CBR) \tag{3}$$

To evaluate the regression model expressed in Equation (3), Table 5 which contains amounts of installation damage reduction factor of geotextiles (RF_{ID}) obtained by tests results and empirical equations and also, the values of residual (difference between the predicted and observed values) is presented. It can be distinguished that in most of the cases, the value of residual for (RF_{ID}) was around 0.05. By comparing the results of tests and regression models, it was distinguished that the coefficient of determination obtained was about 0.21. Also, the standard error of the installation damage reduction factor (RF_{ID}) was about 8%. This clarifies that proposed model with the probability of 92% is significant and reliable.

4. Design graphs and discussion

Based on the established Equation (3), data have been produced and shown in Figures 5–10, to estimate installation damage reduction factor of geotextiles (RF_{ID}) respect to variation of the studied parameters. The design graphs are adjusted to the geotextiles with as-received grab tensile strength equal to 1.35, 0.8 and 0.65 kN, correspond to GT_1, GT_2 and GT_3, respectively. Table 6 is presented to describe what conditions are considered to each design graph.

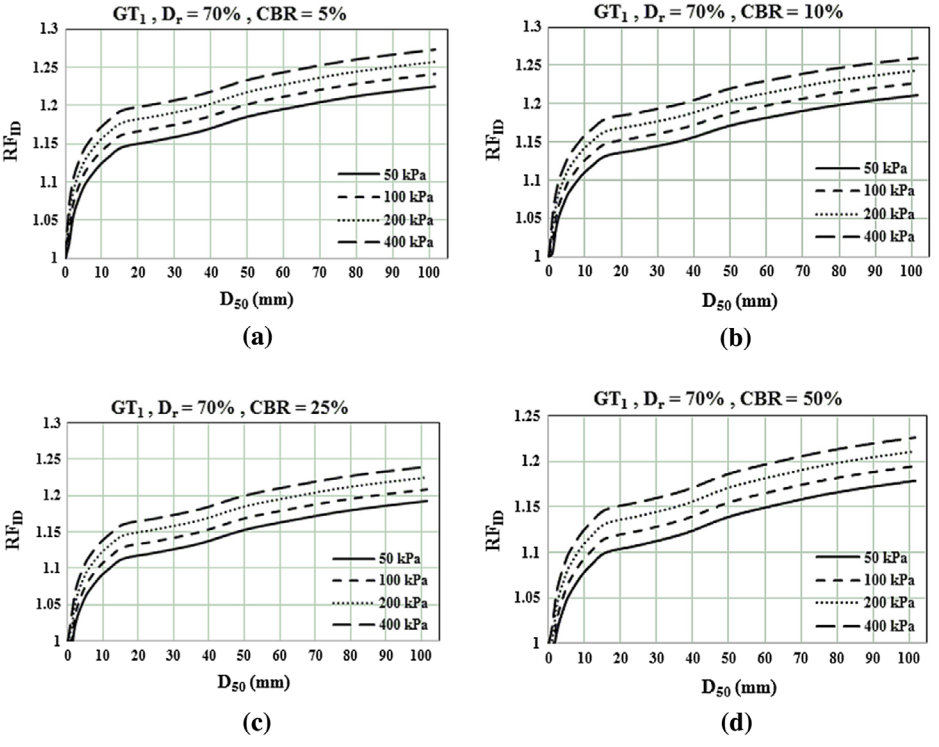

Figure 5. Installation damage reduction factor of geotextiles with class 1 at D_r = 70%.

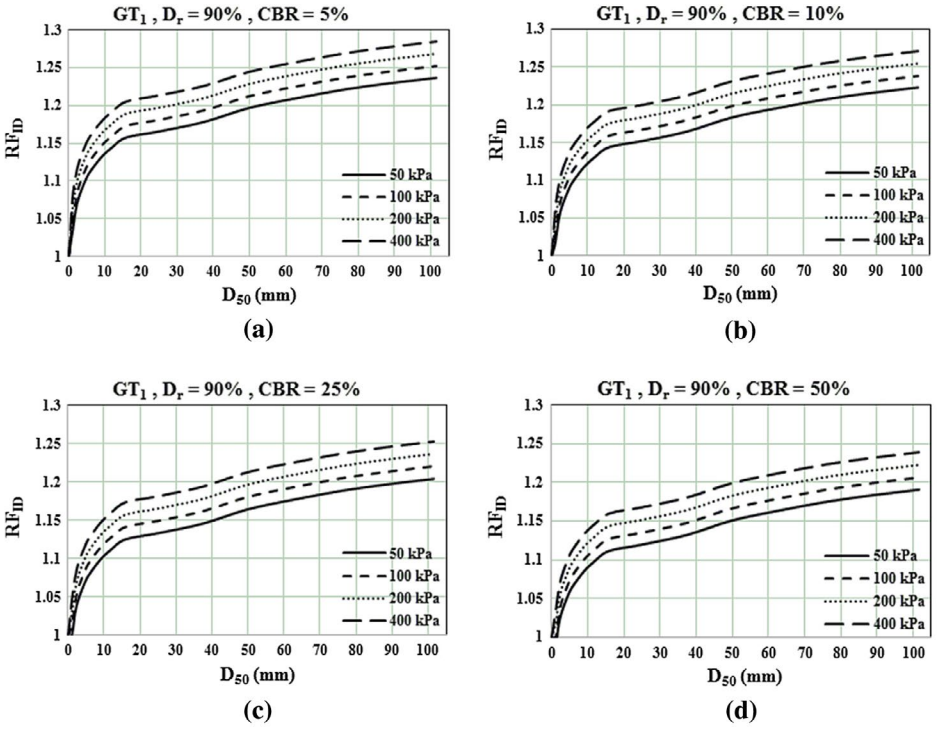

Figure 6. Installation damage reduction factor of geotextiles with class 1 at D_r = 90%.

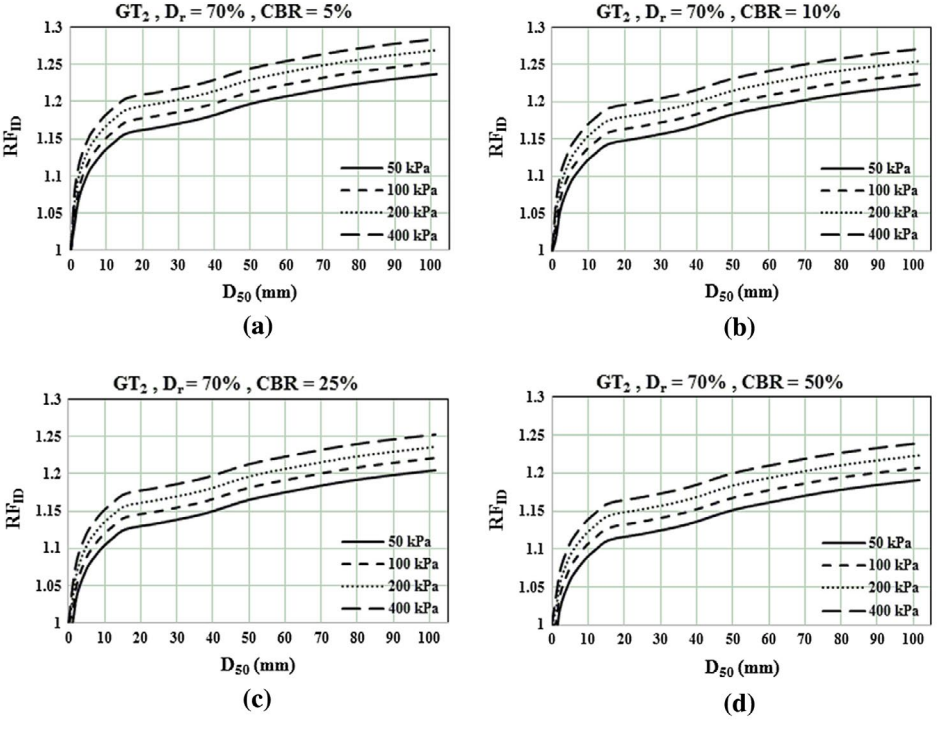

Figure 7. Installation damage reduction factor of geotextiles with class 2 at D_r = 70%.

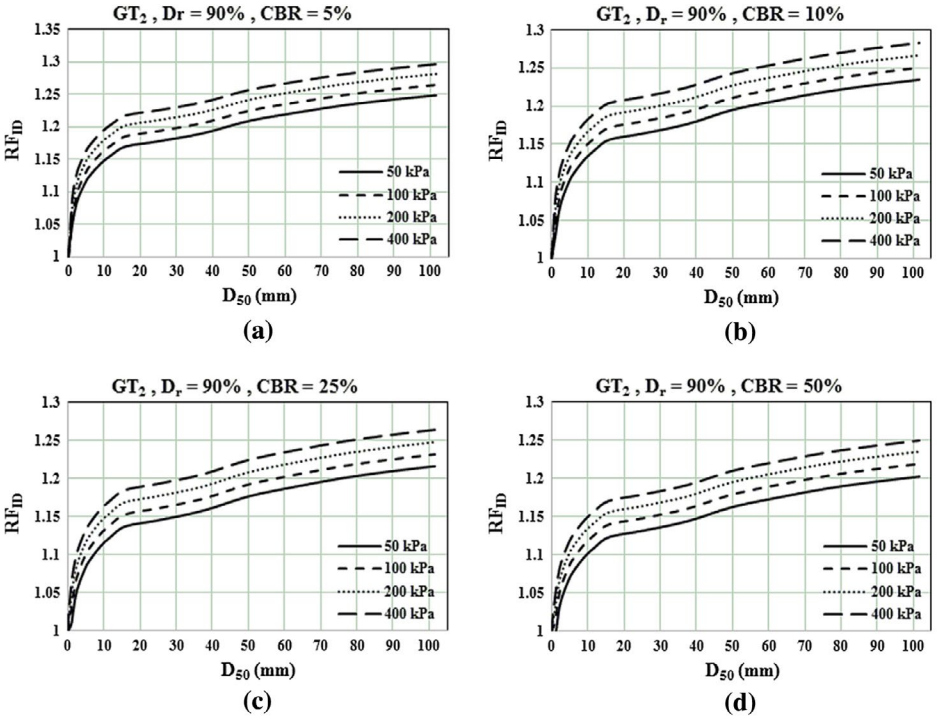

Figure 8. Installation damage reduction factor of geotextiles with class 2 at D_r = 90%.

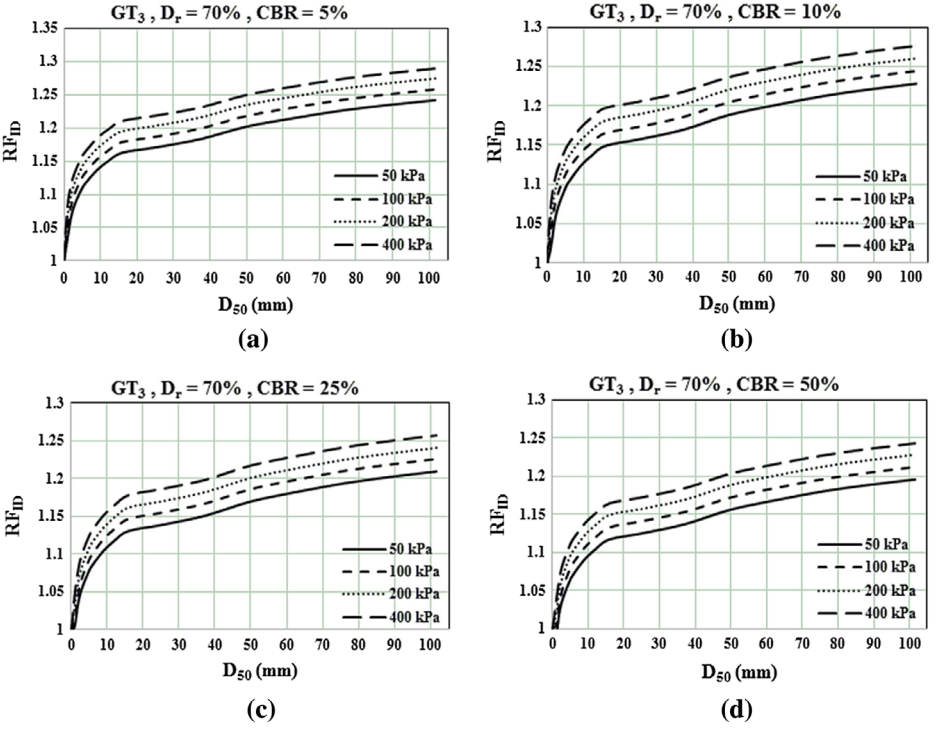

Figure 9. Installation damage reduction factor of geotextiles with class 3 at D_r = 70%.

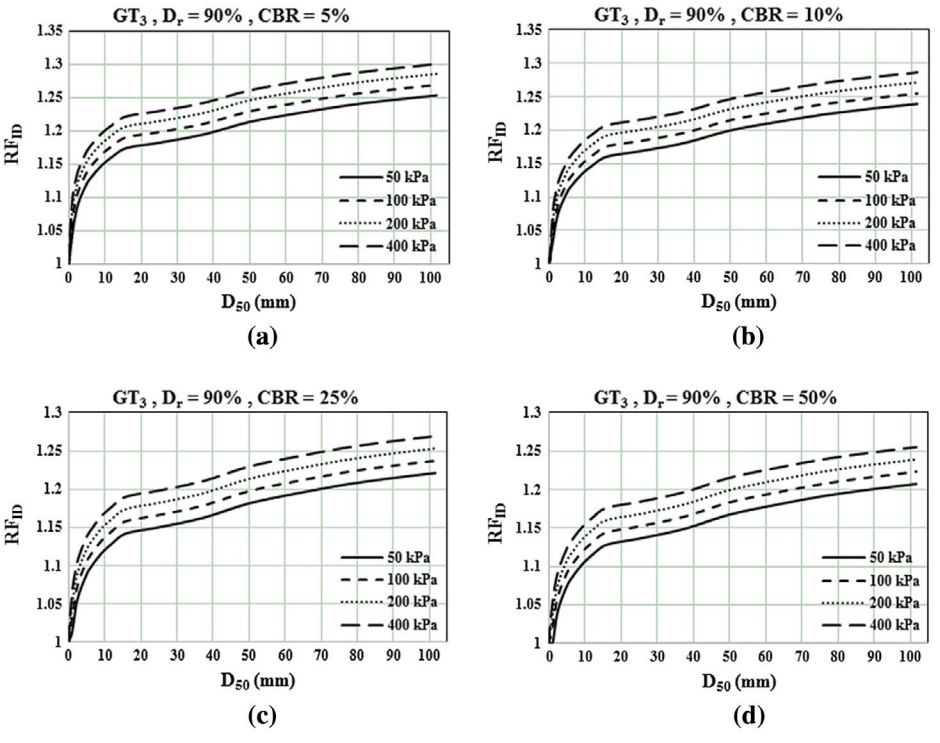

Figure 10. Installation damage reduction factor of geotextiles with class 3 at D_r = 90%.

Table 6. Guidance for using design graphs of installation damage reduction factor of geotextiles (RF_{ID}).

	Relative density of backfill materials, D_r (%)	
Geotextile Class	70	90
GT_1	Figure 5	Figure 6
GT_2	Figure 7	Figure 8
GT_3	Figure 9	Figure 10

Accordingly, reduction factors due to installation of geotextiles in the backfill were obtained 1~1.35. This range of values is in the line with that stated in Berg, Christopher, and Samtani (2009) suggesting RD_{ID} = 1.1~1.4 for nonwoven geotextiles in backfill with maximum grain size 20 mm. As can be seen, increasing the soil particle size intensifies the installation damage of the geotextiles. In fact, increasing the grain size could increase the chance of stone–stone interactions, tending to transfer more stress onto the geotextiles. Expectedly, geotextile class 1 due to its greater thickness, gained less impact from the installation process. Therefore, using high-survivability geotextiles (i.e. class 1 per AASHTO M288–08) in backfills containing large particle size is highly recommended. In this regard, Berg et al. (2009) focused on the grain size of backfill and geotextiles type to suggest reduction factor due to installation damage. From Figures 5–10, it is remarkable that the transferred stress on the geotextile level is one of the most destructive factors on geotextiles survivability. The transferred stress at the level of geotextile can be the resultant of the backfill's weight and stress propagated by the compactor energy, having direct role in installation damage. Consequently, it is suggested that in constructions, lighter compactors and thicker cover of the backfill materials over the geotextile should be utilised, as much as possible. This has been found out by Greenwood and Brady (1992); Watts and Brady (1994); Watn et al. (1998); Elvidge and Raymond (1999); Pinho-Lopes and Lopes (2013); Hufenus, Rüegger, Flum, and Sterba (2005). Based on Equation (3) and regard to Figures 5–10, it is obvious that medium grain size of the backfill with order of two, in compared with transferred stress with order of

one, has more significant effect on the installation damage of geotextiles. Furthermore, the results confirm continued degradation of geotextiles in the aftermath of being in the neighbourhood of weaker subgrades. Actually, weak subgrade directly affects on the amount of extension in the geotextile layer under imposed stress. It means that reduction in CBR of the subgrade ended in occurrence of more settlements beneath the geotextile, exerting more tension through its plane and thereby causing severe damage. Holtz et al. (1998) recommends that higher survivability geotextiles should be used when the subgrade has low shear strength.

Eventually, increasing the relative density of backfill materials increased the installation damage reduction factor because by increasing both of the weight of backfill materials at constant volume and the number of roller passes, cause applied the more energy on geotextile and thus decreased the tensile strength. Also, it can be concluded that the variations of installation damage reduction factors of geotextiles due to transferred stress and relative density are of the same order.

5. Summary and conclusions

The geotextile strength required to survive the most severe conditions anticipated during construction. This paper particularly relates the construction elements including grain size and density of backfill materials, subgrade strength, geotextile strength and the transferred stress over the geotextiles to damage rate of the geotextile. The results were presented based on a series of full-scale field tests and analytical procedures and the outputs were displayed in the form of reduction factor of nonwoven geotextiles due to installation process. The proposed relationships can be useful to estimate the reduction factor for nonwoven geotextiles, providing some sort of reliable data.

The results confirmed that, irrespective to the geotextiles' class, the tensile strength and the failure strain of geotextiles after installation attenuated. In other hand, the geotextiles got stiffer as they were elongated during the tensile tests. Also, it was observed that the medium grain size of the backfill highly affected the retained tensile strength of the geotextiles. Furthermore, increase in transferred stress on the geotextiles due to increasing weight of backfill over the geotextile or/and increasing the number of compactor weight and passes, resulted in the retained tensile strength weaken. The subgrades' CBR is another wrecking factor in installation damage of the geotextiles due to its direct effect on the amount of extension in the geotextile layer under imposed stress. Consequently, the severity of the construction environment should be rectified by selection of geotextiles with higher as-received grab tensile strength (increasing the geotextiles class from 3 to 1) to remediate the installation damage.

Nomenclature

C_u	Coefficient of uniformity
C_c	Coefficient of curvature
D_{50}	Medium grain size
G_s	Specific gravity of soil
CS	Coarse-grained subgrade
FS	Fine-grained subgrade
T_0	As-received grab tensile strength of the geotextiles
σ	Transferred stress at the level of geotextile
D_r	Backfill's relative density
CBR	Subgrade' CBR
R	Ratio of retained strength of geotextile
RF_{ID}	Installation damage reduction factor of geotextile
T_{ID}	Retained grab tensile strength of the geotextiles
$T_0 / (\sigma D_{50}^2)$	Dimensionless parameter
J_{ID}	Retained secant modulus of the geotextiles
J_0	As-received secant modulus of the geotextiles

Disclosure statement

No potential conflict of interest was reported by the authors.

References

Allen, T. M., & Bathurst, R. J. (1994). Characterization of geosynthetic load-strain behavior after installation damage. *Geosynthetics International, 1*, 181–199.

American Association of State Highway and Transportation Officials. (2008). *Standard Specification for Geotextile Specification for Highway Applications*. Virginia, VA, USA: AASHTO M288–08.

American Society for Testing and Materials. (2015). *Standard Test Method for Grab Breaking Load and Elongation of Geotextiles*. ASTM D4632–15.

Becker, L. D. B., & Da silva Nunes, A. L. L. (2015). Influence of soil confinement on the creep behavior of geotextiles. *Geotextiles and Geomembranes, 43*, 351–358.

Carlos, D. M., Pinho-Lopes, M., Carneiro, J. R., & Lopes, M. L. (2015). Effect of soil grain size distribution on the mechanical damage of nonwoven geotextiles under repeated loading. *International Journal of Geosynthetics and Ground Engineering,* 1–9.

Costa, C. M. L., Zornberg, J. G., Bueno, B. D. C., & Costa, Y. D. J. (2016). Centrifuge evaluation of the time-dependent behavior of geotextile-reinforced soil walls. *Geotextiles and Geomembranes, 44*, 188–200.

Berg, R. R., Christopher, B. R., & Samtani, N. C. (2009). *Design of mechanically stabilized earth walls and reinforced soil slopes*, Vol. 1: FHWA NHI-10-024. Washington, DC: Federal Highway Administration.

Elias, V. (2001). *Corrosion/degradation of soil reinforcements for mechanically stabilized earth walls and reinforced soil slopes*, FHWA-NHI-00-044. Washington, DC: Federal Highway Administration.

Elvidge, C. B., & Raymond, G. P. (1999). Laboratory survivability of nonwoven geotextiles on open-graded crushed aggregate. *Geosynthetics International, 6*, 93–117.

Greenwood, J. H., & Brady, K. C. (1992). Geotextiles in aggressive soils. *Construction and Building Materials, 6*, 15–18.

Holtz, R. D., Christopher, B. R., & Berg, R. R. (1998). *Geosynthetic design and construction guidelines*. FHWA-HI-95-038. Washington, DC: Federal Highway Administration.

Hosseinpour, I., Almeida, M. S. S., & Riccio, M. (2015). Full-scale load test and finite-element analysis of soft ground improved by geotextile-encased granular columns. *Geosynthetics International, 22*, 428–438.

Hufenus, R., Rüegger, R., Flum, D., & Sterba, I. J. (2005). Strength reduction factors due to installation damage of reinforcing geosynthetics. *Geotextiles and Geomembranes, 23*, 401–424.

Koerner, G. R., & Koerner, R. M. (1990). *The installation survivability of geotextiles and geogrids*. Fourth International Conference on Geotextiles, Geomembranes and Related Products, (pp. 597–602), Den Haag.

Mendes, M. J. A., Palmeira, E. M., & Matheus, E. (2007). Some factors affecting the in-soil load–strain behaviour of virgin and damaged nonwoven geotextiles. *Geosynthetics International, 14*, 39–50.

Nikbakht, M., & Diederich, R. (2008). The energy potential and its integration in the national European specification. *Foundations of Civil and Enviromental Engineering,* 41–53.

Pinho-Lopes, M., & Lopes, M. L. (2013). Tensile properties of geosynthetics after installation damage. *Enviromental Geotechnics, 1*, 161–178.

Portelinha, F. H. M., Bueno, B. S., & Zornberg, J. G. (2013). Performance of nonwoven geotextile-reinforced walls under wetting conditions: Laboratory and field investigations. *Geosynthetics International, 20*, 90–104.

Portelinha, F. H. M., Zornberg, J. G., & Pimentel, V. (2014). Field performance of retaining walls reinforced with woven and nonwoven geotextiles. *Geosynthetics International, 21*, 270–284.

Richardson, G. N. (1998). Field evaluation of geosynthetic survivability in aggregate road base. *Geotechnical Fabrics Report, 16*, 34–38.

Rosete, A., Mendonça Lopes, P. M., Pinho-Lopes, M., & Lopes, M. L. (2013). Tensile and hydraulic properties of geosynthetics after mechanical damage and abrasion laboratory tests. *Geosynthetics International, 20*, 358–374.

Tavakoli Mehrjardi, Gh., Ghanbari, A., & Mehdizadeh, H. (2016). Experimental study on the behaviour of geogrid-reinforced slopes with respect to aggregate size. *Geotextiles and Geomembranes, 44*, 862–871.

Tavakoli Mehrjardi, Gh., Moghaddas Tafreshi, S. N., & Dawson, A. R. (2013). Pipe response in a geocell reinforced trench and compaction considerations. *Geosynthetics International, 20*, 105–118.

Wang, L., Zhang, G., & Zhang, J. M. (2011). Centrifuge model tests of geotextile-reinforced soil embankments during an earthquake. *Geotextiles and Geomembranes, 29*, 222–232.

Watn, A., Eiksund, G., & Knutson, A. (1998). *Deformation and damage of nonwoven geotextiles in road construction*. Sixth International Conference on Geosynthetics, (pp. 933–938).

Watts, G. R. A., & Brady, K. C. (1994). *Geosynthetics-installation damage and the measurement of tensile strength*. Fifth International Conference on Geotextiles, Geomembranes and Related Products, (pp. 1159–1164), Singapore.